TECHNICAL ARTICLE

CrossMark

Study of the Microstructural Evolution in a 35Ni-25Cr-Nb Heat-Resistant Alloy by Dilatometry and Electron Microscopy

M. H. Sosa Lissarrague[1,2] · S. Limandri[3] · F. Prado[4] · A. C. Picasso[2,5]

Abstract

The dendritic-type microstructure of the 35Ni-25Cr-Nb alloy, in the as-cast condition, consists of an austenitic matrix and two types of eutectic primary carbides; Nb-rich MC type and Cr-rich $M_{23}C_6$ type both present in interdendritic edges and grain boundaries. During aging at 1073 K for different times, $M_{23}C_6$-type secondary carbides precipitate in the matrix while MC-type carbides would transform into a Ni-Nb silicide, known as G-phase ($Ni_{16}Nb_6Si_7$). The microstructure of this alloy was characterized by scanning electron microscopy with X-ray mapping, backscattered and secondary electron images, electron backscatter diffraction, and dilatometry, in order to detect the G-phase and analyze the conditions under which it is present. This undesirable silicide could reduce creep strength since Nb-rich carbide to G-phase transformation improves nucleation of microcracks in the interface between matrix and the silicide. Silicon and nickel were found on the edges of primary Nb-rich carbides in the as-cast condition. This could be indicating that the transformation of this carbide into Ni-Nb silicide is in an incipient stage and it probably occurs from the outside to the inside of the Nb carbide.

Keywords Dilatometry · EBSD · Heat-resistant alloys · G-phase

Introduction

Centrifugal casting heat-resistant alloys of HP series are widely used for pressure vessels, piping, fittings, valves, and other equipments in refineries and petrochemical plants. High resistance to carburization and oxidation of up to 1323 K makes these materials ideal for applications in manufacturing tubes, flanges, cones, harps, headers and coils in furnaces, transfer lines, heaters, and other appliances, for direct reduction in iron ore plants, petrochemical, chemical, and commercial heat treating industries. These materials must satisfy certain conditions such as high mechanical properties, corrosion resistance, and stability of mechanical properties under service at temperatures below 1323 K [1–8]. For this purpose, elements such as niobium, titanium, vanadium, and zirconium are commonly added to improve creep resistance, due to their tendency to form stable precipitates under service conditions. Also, silicon and manganese are added to increase resistance to different degrading atmospheres.

In the as-cast condition, the microstructure of HP-Nb alloys consists of an austenitic matrix with intergranular and interdendritic eutectic-like primary chromium-rich carbides $M_{23}C_6$ type and niobium-rich carbides MC type. During aging, intragranular secondary $M_{23}C_6$ carbides precipitate within the matrix. At operating temperatures, MC-type carbides are thermally unstable, since they would transform into a Ni-Nb silicide, known as G-phase ($Ni_{16}Nb_6Si_7$) [9–11]. For HP-Nb alloy, this transformation is reported to take place between 973 and 1173 K [3, 12, 13]. There is scarce information about this silicide, which is

✉ M. H. Sosa Lissarrague
  mhsl1986@gmail.com

1 Consejo Nacional de Investigaciones Científicas y Técnicas (CONICET), Buenos Aires, Argentina

2 Laboratorio de Metalurgia y Tecnología Mecánica, Universidad Nacional del Sur, 8000 Bahía Blanca, Argentina

3 Facultad de Matemática, Astronomía, Física y Computación, Universidad Nacional de Córdoba and Instituto de Física Enrique Gaviola (IFEG), CONICET, 5000 Córdoba, Argentina

4 Departamento de Física, Universidad Nacional del Sur and IFISUR, CONICET, 8000 Bahía Blanca, Argentina

5 Comisión de Investigaciones Científicas de la Provincia de Buenos Aires (CICPBA), La Plata, Argentina

formed at the interface between the matrix and the niobium carbides and continues inward. This transformation causes an increase in the volume of the unit cell and in the interfacial energy, creating compression stresses on the matrix and tensile stresses on the particles. This fact promotes the nucleation of microcracks, which reduce the creep properties of the alloy [13–17]. In addition, the formation of the G-phase causes a consumption of Ni and Si from the matrix reducing solid solution hardening [15].

The aim of this study is to characterize the microstructural evolution of an HP-Nb alloy during aging at 1073 K at different times from observations by scanning electron microscopy (*SEM*), and electron probe microanalysis with energy-dispersive X-ray spectroscopy (*EDS*). Moreover, it is intended to analyze the conditions under which the transformation of niobium carbides into G-phase takes place, using isothermal dilatometry tests carried out on as-cast samples at 1073, 1098, 1123, and 1148 K.

Experimental Procedure

Specimens of as-cast 35Ni-25Cr-Nb alloy were obtained from a ring extracted from a tube of 110 mm diameter and 11 mm wall thickness and then cut transversely to achieve a 12 mm width.

The chemical composition of the studied material is indicated in Table 1.

Aging treatments were made at 1073 K for different times using resistive furnaces in air atmosphere, and then each aged sample was cooled in air. Samples were ground with silicon carbide papers from 240 to 2000 grit. Polishing was done with 1 μm alumina paste. Polished specimens were electrolytically etched with a 10% KOH aqueous solution at 2 V for 14 s *SEM* and *EBSD* measurements were carried out in a scanning electron microscope with a *Schottky* electron gun. The electron backscatter detector has a camera with 1344×1024 pixels and a 40 mm × 35 mm front phosphor screen. An SDD X-ray detector is also attached to the *SEM* with an 80 mm^2 front area and a nominal resolution of 127 eV for Mn-Kα line (5.893 keV).

Dilatometry measurements were carried out using a vertical design dilatometer fitted with a high-temperature furnace ($300 < T < 1773$ K). The isothermal runs were performed at 1073, 1098, 1123, and 1148 K under argon gas flow of 40 ml min^{-1}. For this purpose, cylindrical specimens of 5 mm diameter and 15 mm length of the as-cast material were used. Experimental data were corrected using Al_2O_3 as standard.

Area fraction measurements of precipitates were performed using the software ImageJ 1.41 over images obtained by optical microscopy at 1000X.

Results and Discussion

Microstructural Characterization of As-Cast Material

SEM images were obtained in the backscattered electron mode (*BSE*) as well as X-ray mapping of elements in the area shown in Fig. 1. Investigation by *SEM* with backscattered electrons (*BSE*) detector showed the presence of a network of precipitates of two types in grain boundaries and interdendritic boundaries which can be distinguished by brightness contrast as dark and bright phases. The difference in the contrast between these phases is due to the fact that niobium has greater atomic weight than chromium [10, 13, 18]. As it can be seen, X-ray mapping shows that dark phases are rich in C and Cr, while bright phases are rich in Ni, Nb, Si, and C. It is interesting to note the presence of a high concentration of Si into bright phases, but not of the dark phases, nor evenly distributed in the matrix is observed, as some authors have found [15, 19]. From the results exposed above, it is possible to confirm that the dark phase is a carbide rich in Cr, while the bright phase is a compound rich in Ni, Nb, and Si. Furthermore, the intergranular and interdendritic precipitates are Cr-rich carbides. However, the techniques we have used do not allow us to determine with certainty the chemical composition of the phases present in the as-cast microstructure. For this purpose, *EDS* analysis was carried out in different areas of the sample in order to identify the chemical composition of both phases, and the results are shown in Table 2. It was found that Cr-rich carbides present a chemical composition that could correspond to both M_7C_3 and $M_{23}C_6$ type (M = Fe, Ni, Cr). On the other hand, several measurements were carried out in bright phases. However, it is not possible to identify with certainty the stoichiometry of this type of compound.

Some authors [6, 7, 18–25], analyzing a similar alloy of the HP family, have pointed out that the as-cast microstructure is composed of an austenitic matrix and a network of primary carbides of the M_7C_3 type (M = Cr, Ni, Fe) and MC type (M = Nb, Ti). During aging at high temperatures, the compound Cr-rich carbides of the M_7C_3 type transform into the $M_{23}C_6$ type and in some cases, it has been observed that the MC-type carbide has transformed into a silicide with stoichiometry $Ni_{16}Nb_6Si_7$, known as G-phase. Another group of authors [5, 26] have found an as-cast

Table 1 Chemical composition of HP-Nb alloy (wt.%)

C	Si	Mn	Cr	Ni	Nb	W	Ti	Fe
0.57	2.73	0.76	23.7	37.6	1.26	0.19	0.07	Bal.

Fig. 1 SEM images of as-cast material in the BSE mode with X-ray mapping
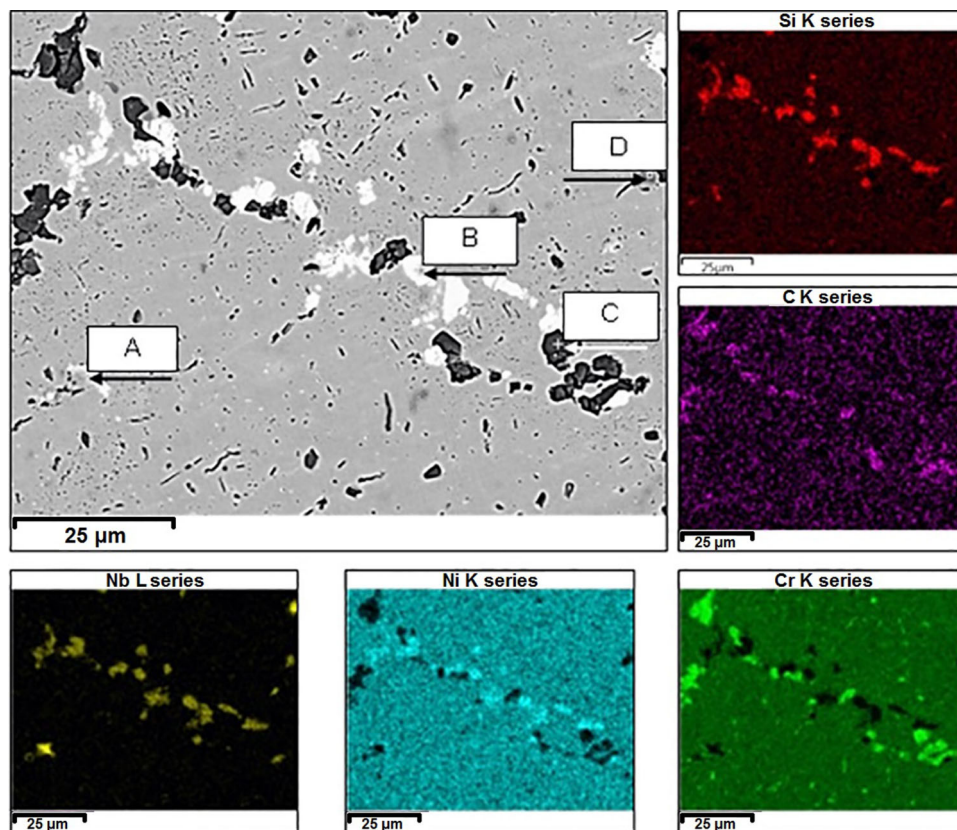
Table 2 Semi-quantitative composition of phases in as-cast condition (at.%)

	C	Ti	Si	Cr	Fe	Ni	Nb
A	15.7	0.5	3.4	19.3	32.5	27.0	1.6
B	19.3	…	6.9	14.8	25.7	29.7	3.5
C	35.9	…	1.9	20.6	23.1	18.5	…
D	…	…	3.4	23.9	40.6	32.1	…

microstructure composed of an austenitic matrix and a network of primary carbides of two types, $M_{23}C_6$ (M = Cr, Ni, Fe) and MC (M = Nb, Ti). Finally, a third group of authors [27] have determined that the microstructure as cast is constituted by an austenitic matrix and a network of primary carbides of three types: M_7C_3 and $M_{23}C_6$ (M = Cr, Ni, Fe), and MC (M = Nb, Ti). In all cases, the compound observed together with the Cr-rich primary carbides in the primary network is the MC-type carbide.

Taking into account what was explained above, and to get more precision in the determination of chemical composition, electron probe microanalysis with *EDS* was carried out in different areas of a bright phase in the as-cast condition (see Fig. 2). Thus, chemical semiquantitative composition was determined on each area, which is presented in Table 3.
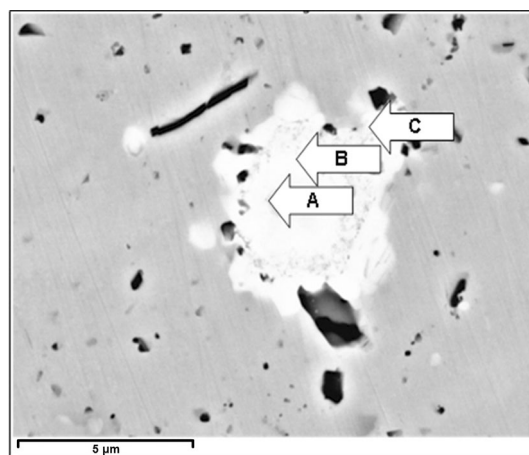

Fig. 2 SEM images in the BSE mode of a bright phase in the as-cast condition

Table 3 EPMA EDS indicating high C, Nb and Ti concentration (at.%)

	C	Ti	Si	Mn	V	Cr	Fe	Ni	Zr	Nb
A	23.0	18.5	1.0	…	0.8	4.4	2.1	3.1	9.5	37.6
B	44.7	13.5	…	…	0.6	2.9	1.2	2.7	4.6	29.7
C	23.6	0.3	17.3	0.2	…	3.7	5.8	36.6	…	12.1

It can be seen that the determined concentrations are in good agreement with X-ray mapping results, i.e., bright phases show high concentration of C and Nb near the core of the particle. Additionally, a determination by micro-analysis performed close to the edge of the phase (C, in Table 3) revealed a high concentration of Si and Ni, which coincides with that observed in the element mapping above. These results are in agreement with those reported by other authors [14, 15, 19].

Similarly, a microanalysis was performed by *EDS* on different areas of the sample over dark particles located in an interdendritic edge (only one measurement is shown), as shown in Fig. 3.

Semiquantitative chemical composition measurements in different dark precipitates in different areas of the sample are shown in Table 4, indicating that those phases are rich in C and Cr.

In order to ensure the identification of those compounds in the as-cast condition, *electron backscatter diffraction (EBSD)* technique was used. In Fig. 4, the *Kikuchi* bands that characterize the phases are presented. Those indicated in yellow correspond to the $Cr_{23}C_6$ carbide, those marked in blue belong to the austenitic matrix, and finally, the pink bands correspond to the NbC carbide.

In contrast to other authors [6, 7, 18–25], the presence of the M_7C_3 primary carbide in the as-cast condition has not been detected in either its hexagonal or its orthorhombic crystal structures.

Therefore, we can confirm that the microstructure in the as-cast condition of the HP-Nb alloy analyzed in this work is composed of an austenitic matrix with a network of Nb-rich primary eutectic carbides surrounded by Si and Ni and Cr-rich carbides of $M_{23}C_6$ type.
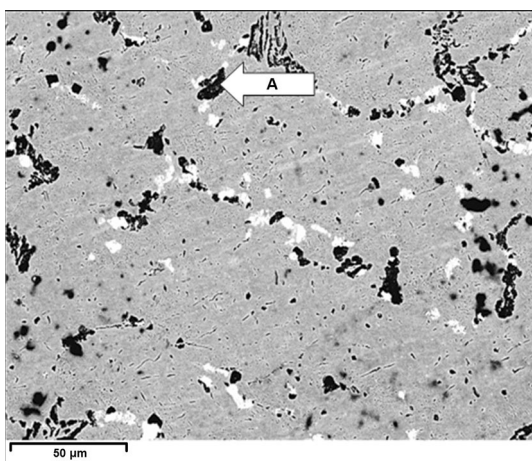
Dilatometry Measurements

Figure 5a shows an isothermal dilatometric curve on which the change in sample length relative to its original length and its first derivate are plotted as a function of time.

In zone B, the contraction rate is the lowest since the derivate reaches a minimum. Finally, the contraction rate first rises and then starts to decrease slowly above 750 min (zone C). This behavior can be explained taking into account the as-cast microstructure of the alloy. The dendritic-type microstructure is intrinsically unstable due to the high cooling rate of the solidification process of these alloys. During solidification, microsegregation of elements such as Ni, Fe, Cr, Si, Mn, and Nb will occur [28]. Under aging conditions at the indicated temperatures, diffusion of elements will occur without changing the dendritic structure. This phenomenon promotes matrix relaxation and could result in a contraction of the sample. For other alloys of dendritic-type microstructure, such as Co-base cast alloys, similar behavior was reported under isothermal dilatometric runs [29]. This behavior can be observed all along the duration of the dilatometric test. However, in superposition with these phenomena, it is possible to note that the curve shows a slope change, in zone B. This change in the contraction rate could be the consequence of a phase transformation in the sample. As it was mentioned above for similar alloys, MC-type carbides under aging at high temperatures transform into a Ni-Nb-rich silicide, known as G-phase of composition $Ni_{16}Nb_6Si_7$. Some authors [19, 30] indicate that this Ni-Nb silicide could be η-phase of composition Nb_3Ni_2Si.

Taking into account that a high concentration of Si and Ni was found around the Nb-rich precipitates, but not in the matrix, the transformation into Ni-Nb-rich silicide would not be gradual, since the time needed for the diffusion of the Si and Ni atoms to form the precipitate decreases with respect to when the atoms must travel through the matrix toward the precipitate. This would result in a higher transformation rate.

The G-phase unit cell has a lattice parameter of 1.12 nm [31], while NbC has a lattice parameter of 0.44 nm, that is,

Fig. 3 SEM images in the BSE mode of dark phases in the as-cast condition

Table 4 EPMA EDS indicating high C, and Cr concentration (at.%)

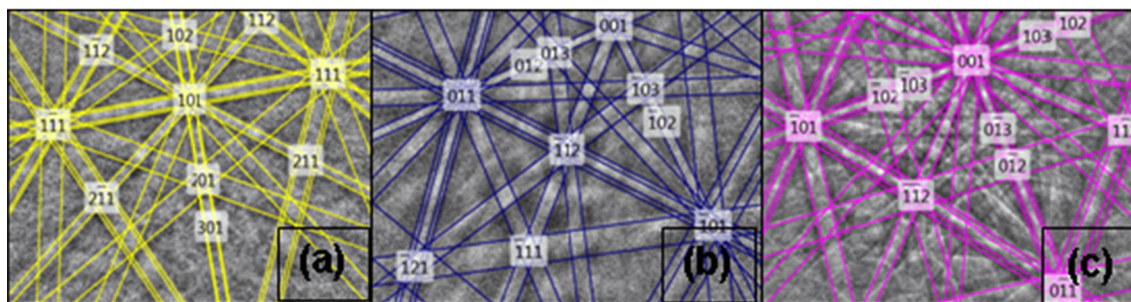|	C	Cr	Fe	Ni
A	25.3	66.7	5.1	2.8
B	24.9	66.9	4.9	3.2
C	24.8	66.7	5.2	3.1
D	24.8	65.3	6.1	3.7
E	25.0	66.4	5.2	3.2
F	24.7	66.9	5.7	2.5
G	24.7	66.3	6.0	2.9
Media	24.9	66.5	5.5	3.1

Fig. 4 Kikuchi bands of the phases in the as-cast condition alloy: (**a**) Cr23C6 carbide, (**b**) austenitic matrix, and (**c**) NbC carbide
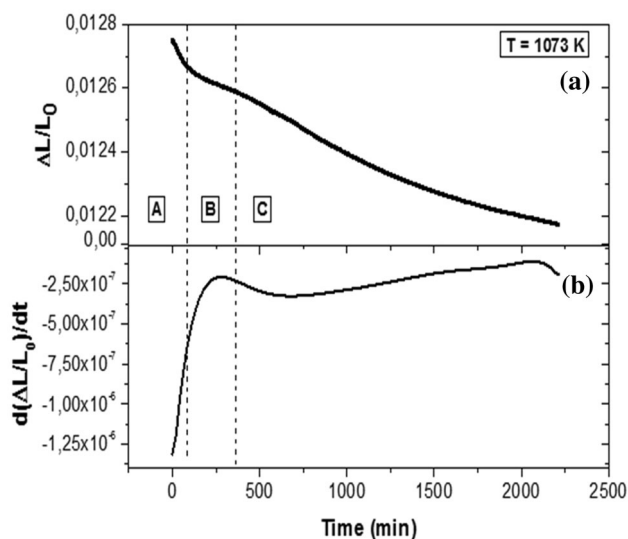

Fig. 5 Isothermal dilatometric run at 1073 K: (**a**) relative length change vs. time and (**b**) first derivate of relative length change vs. time

Fig. 6 Isothermal dilatometric run at 1098 K that shows relative length change vs. time

2.5 times lower. Thus, the NbC unit cell volume is 16.5 times lower than the G-phase unit cell. This fact, in addition to the contraction of the sample, should indicate a decrease in the contraction rate as shown in Fig. 5 (zone B); in spite of the low volume fraction, the decrease in the contraction rate observed in the dilatometry curve (zone B), suggests that the new phase becomes unstable at this temperature and for these times and dissolves.

In Fig. 6, the relative expansion as a function of time is shown at a constant temperature of 1098 K. As it can be seen, similarly to the previous case, the sample undergoes a significant contraction at the beginning of the isothermal stage of the test. It is interesting to note that, unlike the previous case (see Fig. 5), a decrease in the contraction rate at the beginning is not observed. This seems to be an indication that at this temperature, the transformation of the NbC into the G-phase would not occur. It is observed that during the complete dilatometric test, the relative length change decreases gradually until 5000 min, when it approaches a constant value.
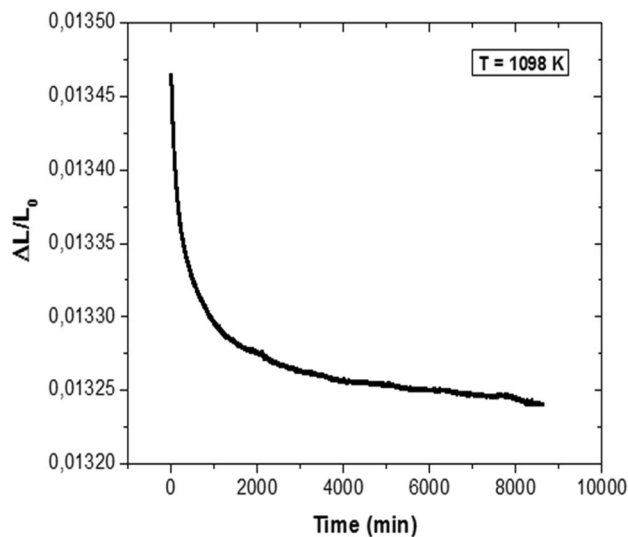
In Fig. 7, the relative expansion as a function of time is shown at a constant temperature of 1123 K. As it can be seen, and analogously to the previous case, the sample undergoes a contraction at the beginning of the isothermal stage of the test (between 0 and 250 min, approximately). Such a behavior is associated with the microsegregation phenomenon, which is faster than in the previous cases because the temperature is higher. In this case, after this initial period, the sample undergoes a sustained expansion between 500 and 3000 min. After this time, the expansion rate increases until practically stabilized. This sustained expansion of the material could be indicating that the transformation of the Nb carbide into the G-phase may be stable at this temperature.

In Table 5, several area fraction measurements on samples aged at 1073 and 1123 K for different times are shown. It was found that the amount of secondary Cr-rich precipitates increases with respect to the as-cast condition, which would not affect the behavior observed previously in the dilatometry curves at 1073 and 1123 K (see Figs. 5 and 7), since both of them have an opposite behavior to each other.
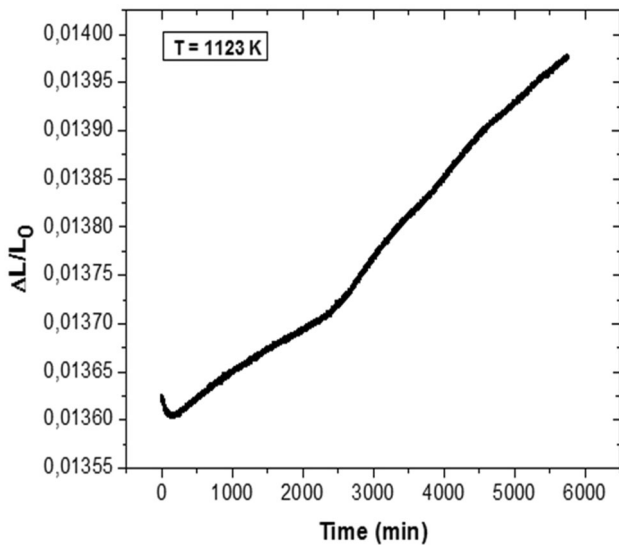
Fig. 7 Isothermal dilatometric run at 1123 K that shows relative length change vs. time

Table 5 Percentage of area fraction of secondary Cr-rich carbides

	As-cast	2 h	5 h	24 h	48 h
1073 K	1.8	4.2	4.1	5	…
1123 K	1.8	…	…	…	3.1

In Fig. 8, the relative expansion as a function of time is shown for a constant temperature of 1148 K. As in the previous case, the sample undergoes a contraction at the beginning of the isothermal stage, due to the microsegregation phenomenon. Because of the higher temperature of the test, the initial behavior is much faster in the present
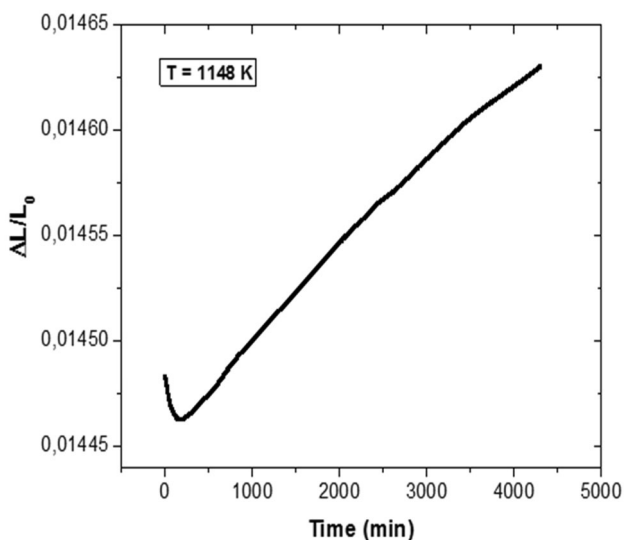

Fig. 8 Isothermal dilatometric run at 1148 K that shows relative length change vs. time

case. A sustained and practically constant expansion is observed over time. This behavior is similar to the previous cases in which the transformation of the Nb carbide into the G-phase is stable at this temperature.

Conclusions

From the characterization of the microstructural evolution of the 25Cr-35Ni alloy, it is possible to reach the following conclusions:

1. The microstructure of an HP-Nb alloy in its as-cast condition consists of an austenitic matrix with primary eutectic Nb-rich carbides of MC-type and Cr-rich carbides of $M_{23}C_6$-type network in grain boundaries and interdendritic edges.
2. The contraction observed in the sample at the first stage of the isothermal dilatometric runs at high temperatures could be an indication that the microstructure undergoes chemical homogenization. This phenomenon would contribute to counteract the effect of the microsegregation of chemical elements in the matrix and in the interdendritic edges.
3. The transformation of Nb carbide into the Ni-Nb silicide induces a significant volume change in the unit cell. This effect is manifested during the isothermal dilatometry tests at the temperatures at which the sample shows an expansion.
4. The increase in the area fraction of secondary Cr-rich carbides does not cause an isothermal expansion or contraction of the sample on the dilatometry tests. The area fraction increases during aging both at 1073 and at 1123 K, but the sample contracts and expands isothermally, respectively.

References

1. D.B. Roach, J.A. Van Echo, Comparison of the properties of the HK-40 and HP-45 cast heat-resistant alloys. Stainl. Steel Cast. ASTM STP **756**, 275–312 (1982). https://doi.org/10.1520/STP28447S
2. W.T. Hou, R.W.K. Honeycombe, Structure of centrifugally cast austenitic stainless steels: part 1 HK40 as cast and after creep between 750 °C and 1000 °C. Mater. Sci. Technol. **1**, 385–389 (1985). https://doi.org/10.1179/mst.1985.1.5.385
3. M.C. Blair, *Cast Stainless Steels. Metals Handbook*, vol. 1 (ASM, Materials Park, 1982)
4. X. Zhang, D. Kong, Chemical composition design and mechanical properties of a modofied HP-type heat-resistant alloy. J. Mater. Sci. **3**, 124–127 (2013)
5. E.A. Kenik, P.J. Maziasz et al., Structure and phase stability in a cast modified-HP austenite after long-term ageing. Scr. Mater. **49**, 117–122 (2003). https://doi.org/10.1016/S1359-6462(03)00238-0

6. J. Laigo, F. Christien et al., SEM, EDS, EPMA-WDS and EBSD characterization of carbides in HP type heat resistant alloys. Mater. Charact. **59**, 1580–1586 (2008). https://doi.org/10.1016/j.matchar.2008.02.001

7. K. Buchaman, M. Kral, C. Bishop, Crystallography and morphology of MC carbides in Niobium–Titanium modified as-cast HP alloys. Metall. Mater. Trans. A **45A**, 3373–3385 (2014). https://doi.org/10.1007/s11661-014-2285-2

8. D.J. Tillack, J.E. Guthrie, Wrought and cast heat-resistant stainless steels and nickel alloys for the refining and petrochemical industries. Nickel Development Institute. Technical Series No. 10071 (1998)

9. D. Knowles, C. Thomas, D. Keen, Q. Chen, In service embrittlment of cast 20Cr32Ni1Nb components used in steam reformer applications. Int. J. Press. Vessels Pip. **81**, 499–506 (2004). https://doi.org/10.1016/j.ijpvp.2003.12.025

10. S. Shi, J.C. Lippold, Microstructure evolution during service exposure of two cast, heat-resisting stainless steels HP-Nb modified and 20-32Nb. Mater. Charact. **59**, 1029–1040 (2008). https://doi.org/10.1016/j.matchar.2007.08.029

11. M.P. Dewar, A.P. Gerlich, Correlation between experimental and calculated phase fractions in aged 20Cr32Ni1Nb austenitic stainless steels containing nitrogen. Metall. Mater. Trans. A **44**, 627–639 (2013)

12. M. Garbiak, R. Chylinska, Precipitation kinetics in austenitic 18Cr–30Ni–Nb cast steel. Arch. Foundry Eng. **8**, 27–30 (2008)

13. L.H. de Almeida, A. Freitas Ribeiro, I. Le May, Microstructural characterization of modified 25Cr–35Ni centrifugally cast steel furnace tubes. Mater. Charact. **49**, 219–229 (2003). https://doi.org/10.1016/S1044-5803(03)00013-5

14. L.H. de Almeida, P.R.O. Emygdio, I. Le May, F.C. Ferraz, Microstructural characterization and geometrical analysis of welded joints of high temperature stainless steel tubes, in *Microstructural Science, Vol. 24: Understanding Microstructure: Key to Advances in Materials*, ed. by M.G. Burke, E.A. Clark, E.J. Palmiere (ASM, Materials Park, 1996), pp. 193–198

15. X. Guo, X. Jia, J. Gong et al., Effect of long-term aging on microstructural stabilization and mechanical properties of 20Cr32Ni1Nb steel. Mater. Sci. Eng. A **690**, 62–70 (2017). https://doi.org/10.1016/j.msea.2017.02.057

16. C.J. Liu, Y. Chen, Variations of the microstructure and mechanical properties of HP40Nb hydrogen reformer tube with time at elevated temperature. Mater. Des. **32**, 2507–2512 (2011). https://doi.org/10.1016/j.matchar.2008.02.001

17. R.C. Ecob, R.C. Lobb, V.L. Kohler, The Formation of G-phase in 20/25 Nb stainless steel AGR fuel cladding alloy and its effect on creep properties. J. Mater. Sci. **22**, 2867–2880 (1987)

18. R.A.P. Ibañez, G.D. de Almeida Soares, L.H. de Almeida, I. Le May, Effects of Si content on the microstructure of modified-HP austenitic steels. Mater. Charact. **30**, 243–249 (1993)

19. A. Alvino, D. Ramires, A. Tonti, D. Lega, Influence of chemical composition on microstructure and phase evolution of two HP heat resistant stainless steels after long term plant-service aging. Mater. High Temp. **31**(1), 1–11 (2014). https://doi.org/10.1179/0960340913Z.0000000001

20. A.R. Andrade, C. Bolfarini, L.A.M. Ferreira et al., Titanium micro addition in a centrifugally cast HPNb alloy: high temperature mechanical properties. Mater. Sci. Eng. A **636**, 48–52 (2015). https://doi.org/10.1016/j.msea.2015.03.085

21. C.J. Liu, X.D. Chen et al., Phase transformation of Nb in carburized zone of 25Cr–35Ni–Nb+ MA alloy after service. Proc. Eng. **130**, 693–700 (2015). https://doi.org/10.1016/j.proeng.2015.12.165

22. S.Y. Kondrat'ev, V.S. Kraposhin et al., Experimental observation and crystallograpfic description of M_7C_3 carbide transformation in Fe–Cr–Ni–C HP type alloy. Acta Mater. **100**, 275–281 (2015). https://doi.org/10.1016/j.actamat.2015.08.056

23. R. Voicu, E. Adrieu et al., Microstructure evolution of HP40-Nb alloys during aging under air at 1000 °C. Mater. Charact. **60**, 1020–1027 (2009). https://doi.org/10.1016/j.matchar.2009.04.007

24. A.R. Andrade, C. Bolfarini, L.A.M. Ferreira et al., Influence of niobium addition on the high temperature mechanical properties of a centrifugally cast HP alloy. Mater. Sci. Eng. A **628**, 176–180 (2015). https://doi.org/10.1016/j.msea.2015.01.049

25. M. Attarian, A. Karimi Taheri, Microstructural evolution in creep aged of directionally solidified heat resistant HP-Nb steel alloyed with tungsten and nitrogen. Mater. Sci. Eng. A **659**, 104–118 (2016). https://doi.org/10.1016/j.msea.2016.02.046

26. M. Mostafei, M. Shamanian, A. Saatchi et al., Effect of aging temperature on structural evolution of HP-Nb heat resistant steel. Int. J. ISSI **6**(1), 30–33 (2009)

27. A.C. McLeod, C.M. Bishop, K.J. Stevens et al., Microstructure and carburization detection in HP alloy pyrolysis tubes. Metalogr. Microstruct. Anal. **4**, 273–285 (2015). https://doi.org/10.1007/s13632-015-0210-8

28. M. Attarian, A. Karimi Taheri, N. Varahram, P. Davami, Microstructure and segregation behavior of directionally solidified tungsten bearing 25Cr–35Ni–Nb heat-resistant stainless steels. Int. J. Cast Met. Res. (2016). https://doi.org/10.1080/13640461.2016.1261519

29. P. Berthod, C. Heil, L. Aranda, Influence of the morphologic evolution of the eutectic carbides at high temperature on the thermal expansion behavior of refractory cast alloys. J. Alloy. Compd. **504**, 243–250 (2010). https://doi.org/10.1016/j.jallcom.2010.05.101

30. Q.Z. Chen, C.W. Thomas, D.M. Knowles, Characterization of 20Cr32Ni1Nb alloys in as-cast and ex-service conditions by SEM, TEM and EDX. Mater. Sci. Eng. A **374**, 398–408 (2004). https://doi.org/10.1016/j.msea.2004.03.038

31. T. Sourmail, Precipitation in creep resistant austenitic stainless steels. Mater. Sci. Technol. **17**, 1–14 (2001). https://doi.org/10.1179/026708301101508972